

Perpendicular mesoporous Pt thin films: electrodeposition from titania nanopillars and their electrochemical properties†

Satoshi Tominaka,^a Chia-Wen Wu,^{‡b} Toshiyuki Momma,^c Kazuyuki Kuroda^b and Tetsuya Osaka^{*b}

Received (in Cambridge, UK) 25th February 2008, Accepted 17th March 2008

First published as an Advance Article on the web 21st April 2008

DOI: 10.1039/b803225d

A perpendicular mesoporous platinum electrode with a flat surface is successfully synthesized by electrodeposition using titania nanopillars as template, and the electrochemical studies indicate that this material is a promising catalytic electrode for fuel cells because of its high surface area and perpendicular nanopores.

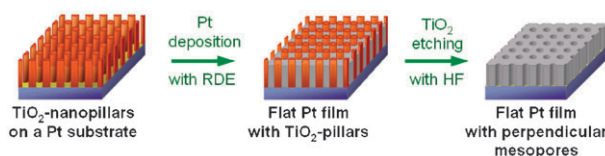
Porous Pt electrodes are an essential component for electrochemical devices such as fuel cells^{1,2} and sensors,^{3,4} and thus the preparation of electrodes with an optimal structure is important. Different synthetic processes have been utilized for producing Pt electrodes with various porous structures. For example, mesoporous Pt with cylindrical pores parallel to the substrate are synthesized by reduction of metal ions dissolved in the aqueous domains of lyotropic liquid crystalline (LLC) phase.^{2,5} Three-dimensionally ordered macroporous (3DOM) Pt electrodes are synthesized by means of colloidal crystal templating.⁶ These porous electrodes have advantages over particles-based electrodes because of their ordered porous nanostructure with relatively large surface area (e.g., ca. 20–50 m² g⁻¹ for mesoporous Pt).^{2,4,5} The ordered structures are useful for precise analyses and the optimization of mass- and ion-transfers in the pores. The large surface promotes reactions on the electrode, and thus the electric current from fuel cells and sensors increases. In particular, perpendicularly-oriented pores exhibit good accessibility from film surfaces and therefore should increase the mass- and ion-transfers.⁷ However, the lack of concurrent achievement of large surface area comparable to nanoparticles (>10 m² g⁻¹) and perpendicularly-oriented porosity greatly reduces the merit.⁷ Perpendicular porous metals (e.g., Pt, Ni, Au) have only been fabricated by means of anodic-alumina replication so far, but the pore sizes of these electrodes are

generally large (in the range of sub-micrometers)⁸ for the application to fuel cells and sensors.

Here we propose a new method for fabricating mesoporous Pt films with uniform pores (ca. 10 nm), perpendicular alignment, and large surface area by electrodeposition using titania nanopillars as template (Scheme 1). In addition, the electrochemical study of the Pt film indicates the potential application as electrodes in fuel cells. Moreover, we expect that such electrodes with a well-defined pore structure is useful for precise analyses on the reactions of fuel cells and sensors.

The fabrication process of the perpendicular mesoporous Pt film is illustrated in Scheme 1. First, the film of titania nanopillars was prepared by following our previous procedure.⁹ A precursor solution containing titanium tetraisopropoxide (TTIP), a surfactant Pluronic P123, ethanol, and HCl_(aq.) was prepared and then spin-coated onto Pt-sputtered Si substrates. The as-coated films were aged at -20 °C for 24 h, and then were heated up to 400 °C (1 °C min⁻¹) and kept at 400 °C for 4 h. Observation with scanning electron microscopy (SEM) confirmed that arrays of nanopillars with an ordered interval of pores around 16 nm were formed on a Pt substrate as shown in Fig. 1(A–C). We previously reported the nanopillars were generated from aggregation of crystalline titania nanoparticles.⁹ The same structure can also be prepared on indium tin oxide (ITO) substrates (ESI†), thus this process is applicable to various electrodes. The characterization of the pore (porosity, surface area, etc.) was performed by water vapor adsorption–desorption isotherms (ESI†).¹⁰ The film of titania nanopillars exhibits a high porosity (ca. 34%) and a flat surface over large area. These properties are beneficial to the replication of the structure by electrodeposition.

Next, we electrodeposited Pt into the film of titania nanopillars, and the optimal condition was found at 0.35 V vs. Ag/AgCl in 10 mM H₂PtCl₆ for 2250 s using a rotating-disc-electrode (RDE) system at 1500 rpm in order to obtain a flat surface.^{11,12} Because titania is inert at the potential 0.35 V,¹³ Pt is deposited only from the Pt substrate to fill out the space of the template. It has been reported that the mass transfer of bulky anionic species (e.g. Fe(CN)₆³⁻) into a mesoporous



Scheme 1 Schematic flow diagram for preparing flat Pt electrodes with perpendicular mesopores.

^a Graduate School of Science and Engineering, Waseda University, Okubo 3-4-1, Shinjuku, Tokyo, 169-8555, Japan

^b Faculty of Science and Engineering, Waseda University, 3-4-1 Okubo, Shinjuku, Tokyo, 169-8555, Japan.

E-mail: osakatets@waseda.jp

^c Waseda Institute for Advanced Study, Waseda University, Nishi-Waseda 1-6-1, Shinjuku, Tokyo, 169-8050, Japan

† Electronic supplementary information (ESI) available: Cyclic voltammograms of titania modified electrodes, water vapor adsorption–desorption isothermal lines of titania nanopillars, additional SEM and TEM images and details of analysis on Fig. 3. See DOI: 10.1039/b803225d

‡ Current address: Department of Chemistry, Iowa State University, Ames, Iowa 50011-3111, USA.

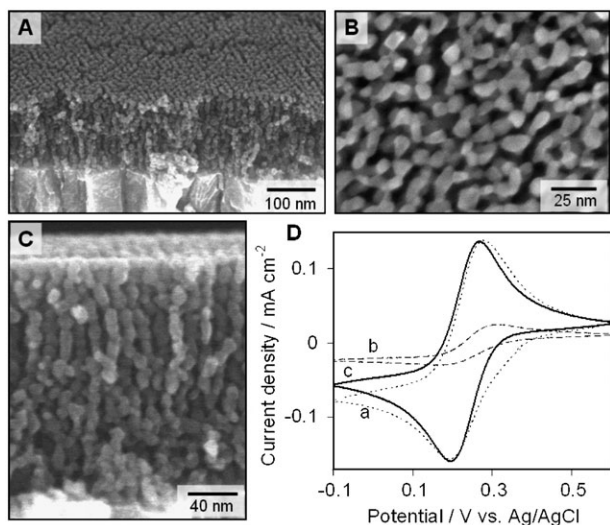


Fig. 1 Characterization of the film of titania nanopillars on conductive substrates; (A–C) SEM images for confirming the generation of the nanopillars on a Pt substrate: (A) a birds-eye view, (B) a top view, and (C) a cross-sectional view. (D) Cyclic voltammograms of $\text{Fe}(\text{CN})_6^{3-}/\text{Fe}(\text{CN})_6^{4-}$ on an indium-tin-oxide (ITO) electrode modified with the mesoporous titania: (a) titania nanopillars calcined at 400 °C, (b) mesoporous titania calcined at 200 °C (before structural transformation to nanopillars, see ESI†), and (c) bare ITO electrode. Scan rate: 50 mV s^{-1} . Electrolyte: 100 mM Na_2SO_4 containing 1 mM $\text{K}_3\text{Fe}(\text{CN})_6$.

titania film was inhibited by electrostatic repulsion between the anion and the titania surface.¹³ Our cyclic voltammetric (CV) results (Fig. 1D) indicate that this phenomenon indeed happened in the case of mesoporous titania film calcined at 200 °C (curve “b”), *i.e.* before the formation of nanopillar structure. However, in the case of the film calcined at 400 °C (curve “a”), *i.e.* after the formation of nanopillar structure, the inhibition was negligible because its CV result is similar to that on a bare electrode (curve “c”).¹³ This study indicates that the nanopillar structure hardly inhibits mass transfer even though the space among the pillars is in the range of several nanometers.¹³

A perpendicular mesoporous Pt electrode was obtained after the removal of the titania nanopillar template. After deposition of Pt, the film of the Pt/TiO₂ composites was soaked in 50% HF aq. for 5 min,¹⁴ washed with a large amount of pure water, and cleaned throughout the electrode surface by an electrochemical hydrogen-evolution process conducted at $-0.25 \text{ V vs. Ag/AgCl}$ for 20 s in a 0.5 M H_2SO_4 . The top and cross-sectional FE-SEM images of the fabricated Pt electrode (Fig. 2A–D) indeed show that the Pt electrode exhibits perpendicular mesopores with an average diameter of *ca.* 10 nm, a flat surface, and a uniform thickness of *ca.* 230 nm for the entire film, indicating a well replicated structure from titania nanopillars. The porosity is estimated as *ca.* 66% according to the porosity of the template when the replication proceeds perfectly. The elemental mapping data by TEM-energy dispersive X-ray spectroscopy (TEM-EDX) indicated that the film was mainly composed of Pt with a small amount of Ti, as shown in Fig. 2E. The black region in the STEM image is confirmed to be mainly composed of Pt, and the white region contains Pt and also Ti. This result indicates

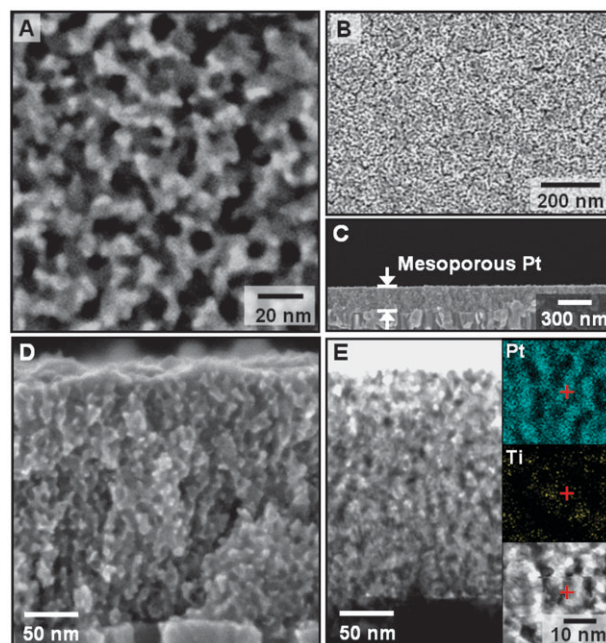


Fig. 2 Electron microscopic characterization of the obtained perpendicular mesoporous Pt electrode: top (A, B) and cross-sectional (C, D) SEM images, and a cross-sectional TEM image (E). The insets in the TEM image were elemental mapping (EDX): Pt–L (top) and Ti–M (middle), and the corresponding STEM image (bottom). The red crosses indicate the same point.

that a small amount of Ti remained as a contaminant in the electrode even after the HF etching.

The electrochemical properties and surface area of the perpendicular mesoporous Pt electrode were evaluated by CV in a sulfuric acid solution (Fig. 3A). The result is well-consistent with a typical CV of polycrystalline Pt electrode, *i.e.* sharp hydrogen ad/desorption current peaks ($-0.1, 0.03 \text{ V}$), constant double-layer-charging current ($0.2\text{--}0.6 \text{ V}$), oxide formation current ($>0.6 \text{ V}$), and oxide deformation current peak (0.6 V).¹⁵ The contaminant (*i.e.*, Ti) had no effect on the CV. We further calculated the roughness factors (R_f) based on the hydrogen-desorption charge,¹⁵ and the R_f value was 50.6 for the perpendicular mesoporous Pt electrode and was 3.8 for a planar (poreless) Pt electrode used as a reference. On the basis of the roughness factor, the thickness, and the density of Pt (21.4 g cm^{-3}), the specific surface area of the obtained Pt electrode was determined as $14.1 \pm 1.4 \text{ m}^2 \text{ g}^{-1}$. This value is smaller than the literature values ($20\text{--}50 \text{ m}^2 \text{ g}^{-1}$) of mesoporous Pt fabricated from LLC processes probably due to larger pores and thicker walls.¹⁶

To use the perpendicular mesoporous Pt electrode as a fuel cell catalyst, we evaluated the oxygen reduction activity of the electrode by hydrodynamic voltammetry (HV).^{17,18} As shown in Fig. 3B, the HVs of the perpendicular mesoporous Pt electrode and a planar Pt electrode were recorded at a rotation rate of 1000 rpm. The results clearly show that there was an increased current density for the mesoporous Pt as compared with that of the planar Pt in the range of the potential between 0.35 to 0.7 V. The increased current is commonly attributed to the large roughness factor of the mesoporous Pt, and also to the possible increase in the inherent catalytic activity. In order

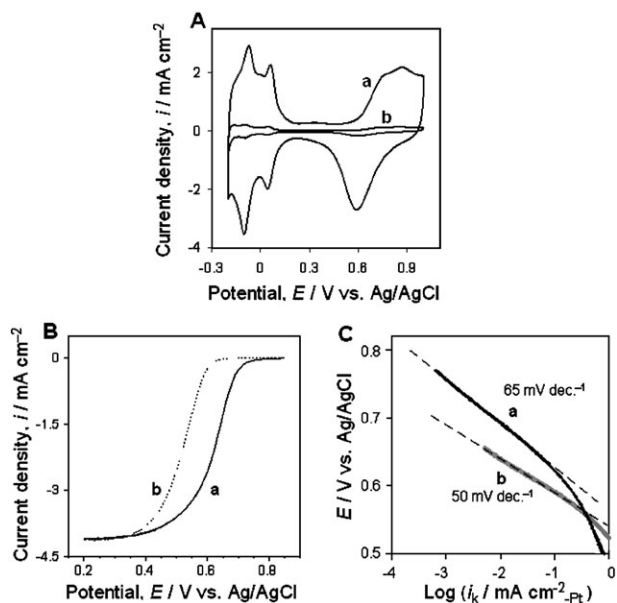


Fig. 3 Electrochemical characterization of (a) the perpendicular mesoporous Pt electrode compared with (b) a planar polycrystalline Pt electrode. (A) Cyclic voltammograms in 0.5 M H₂SO₄ solution saturated with nitrogen at 50 mV s⁻¹. (B) Hydrodynamic voltammograms in oxygen reduction in oxygen saturated 0.5 M H₂SO₄ solution at 25 °C. Rotating rate: 1000 rpm. Scan range: from open-circuit potential to 0.2 V. Scan rate: 1 mV s⁻¹. (C) Diffusion-controlled Tafel plot based on electrochemically-active surface area corresponding to the hydrodynamic voltammograms.

to evaluate the activity, the specific activity defined as current density per electrochemically-active surface area (A_{ec}) is determined from the diffusion-corrected Tafel plot (Fig. 3C). The typical slope of a Tafel plot of oxygen reduction^{17–19} (*i.e.*, ~60 mV decade⁻¹) was obtained, which can explain that the reaction mechanism of oxygen reduction for the perpendicular mesoporous Pt was the same as that for regular Pt electrodes. At 0.7 V, the perpendicular mesoporous Pt exhibits a higher specific activity ($-7.5 \mu\text{A cm}^{-2}_{-Pt}$) than the planar Pt ($-0.61 \mu\text{A cm}^{-2}_{-Pt}$). The specific activity of the perpendicular mesoporous Pt is well-consistent with that ($-7.4 \mu\text{A cm}^{-2}_{-Pt}$) from the mesoporous Pt electrodes made by LLC process.¹⁹ The increased activity compared with the planar Pt can be explained by the difference in microstructure (*e.g.*, crystal size)¹⁸ and/or morphology (*e.g.*, concave structure).²⁰ The high-resolution TEM (HR-TEM) image of the perpendicular mesoporous Pt electrode displayed Pt nanocrystallites with sizes of 5–7 nm in the framework (ESI[†]). This crystal size is much smaller than that of bulk Pt (or the planar Pt electrode). As for the morphological effect, our perpendicular mesoporous Pt electrode possesses a concave structure which has been proved to be able to enhance the catalytic activity of electrode.²⁰

In conclusion, a perpendicular mesoporous Pt film possessing a nanopore size of 10 nm, a flat surface, and a high surface area was synthesized by electrodeposition using titania nanopillars as a template. Moreover, the fabricated mesoporous Pt film showed high oxygen-reduction activity as compared to a planar Pt electrode. This new material is expected to possess

potential applications for electrocatalysts, *e.g.*, oxygen reduction reaction catalysts for fuel cells.

We thank Dr T. Aida (Waseda University) for his support on SEM observation and H. Miyamoto (Hitachi Kyowa Corp.) for his support on TEM observation. This work was partly supported by the Global COE program “Center for Practical Chemical Wisdom” and Encouraging Development Strategic Research Centers Program “Establishment of Consolidated Research Institute for Advanced Science and Medical Care” from the Ministry of Education, Culture, Sports, Science and Technology, Japan.

Notes and references

1. S. Motokawa, M. Mohamedi, T. Momma, S. Shoji and T. Osaka, *Electrochemistry*, 2005, **73**, 346.
2. Y. Yamauchi, H. Kitoh, T. Momma, T. Osaka and K. Kuroda, *Sci. Technol. Adv. Mater.*, 2006, **7**, 438; A. Kucernak and J. Jiang, *Chem. Eng. J.*, 2003, **93**, 81.
3. S. Park, T. D. Chung and H. C. Kim, *Anal. Chem.*, 2003, **75**, 3046.
4. S. A. G. Evans, J. M. Elliott, L. M. Andrews, P. N. Bartlett, P. J. Doyle and G. Denuault, *Anal. Chem.*, 2002, **74**, 1322.
5. G. S. Attard, P. N. Bartlett, N. R. B. Coleman, J. M. Elliott, J. R. Owen and J. H. Wang, *Science*, 1997, **278**, 838; G. S. Attard, C. G. Göltner, J. M. Corker, S. Henke and R. H. Templer, *Angew. Chem., Int. Ed. Engl.*, 1997, **36**, 1315.
6. H. Yan, C. F. Blanford, B. T. Holland, M. Parent, W. H. Smyrl and A. Stein, *Adv. Mater.*, 1999, **11**, 1003; K. M. Kulinowski, P. Jiang, H. Vaswani and V. L. Colvin, *Adv. Mater.*, 2000, **12**, 833; O. D. Velev, P. M. Tessier, A. M. Lenhoff and E. W. Kaler, *Nature*, 1999, **401**, 548.
7. A. Walcarius, E. Sibottier, M. Etienne and J. Ghanbaja, *Nat. Mater.*, 2007, **6**, 602; U. Lee, J. H. Lee, D.-Y. Jung and Y.-U. Kwon, *Adv. Mater.*, 2006, **18**, 2825; Y. Yamauchi, M. Sawada, T. Noma, H. Ito, S. Furumi, Y. Sakka and K. Kuroda, *J. Mater. Chem.*, 2005, **15**, 1137.
8. H. Masuda and K. Fukuda, *Science*, 1995, **268**, 1466; T. Ohmori, T. Kimura and H. Masuda, *J. Electrochem. Soc.*, 1997, **144**, 1286; T. Yanagishita, K. Nishio and H. Masuda, *Adv. Mater.*, 2005, **17**, 2241.
9. C.-W. Wu, T. Ohsuna, M. Kuwabara and K. Kuroda, *J. Am. Chem. Soc.*, 2006, **128**, 4544.
10. C. Boissiere, D. Grosso, S. Lepoutre, L. Nicole, A. B. Bruneau and C. Sanchez, *Langmuir*, 2005, **21**, 12362.
11. A. J. Bard and L. R. Faulkner, *Electrochemical: Methods Fundamentals and Applications*, Wiley, New York, 2000, ch. 9.
12. M. Paunovic and M. Schlesinger, *Fundamentals of Electrochemical Deposition*, John Wiley & Sons, New Jersey, 2nd edn, 2006; S. Motokawa, M. Mohamedi, T. Momma, S. Shoji and T. Osaka, *Electrochem. Commun.*, 2004, **6**, 562; A. M. Feltham and M. Spiro, *Chem. Rev.*, 1971, **71**, 177.
13. M. Etienne, D. Grosso, C. Boissiere, C. Sanchez and A. Walcarius, *Chem. Commun.*, 2005, 4566; M. Etienne, A. Quach, D. Grosso, L. Nicole, C. Sanchez and A. Walcarius, *Chem. Mater.*, 2007, **19**, 844.
14. T. Ohno, K. Sarukawa and M. Matsumura, *J. Phys. Chem. B*, 2001, **105**, 2417.
15. S. S. Kocha, in *Handbook of Fuel Cells: Fundamentals Technology and Applications*, ed. W. Vielstich, A. Lamm and H. A. Gasteiger, John Wiley & Sons, England, 2003, ch. 43; H. Xu, E. Brosha, F. Garzon, F. Uribe, M. Wilson and B. Pivovar, *ECS Trans.*, 2007, **11**, 383; T. R. Ralph, G. A. Hards, J. E. Keating, S. A. Campbell, D. P. Wilkinson, M. Davis, J. StPierre and M. C. Johnson, *J. Electrochem. Soc.*, 1997, **144**, 3845.
16. J. M. Elliott and J. R. Owen, *Phys. Chem. Chem. Phys.*, 2000, **2**, 5653.
17. U. A. Paulus, T. J. Schmidt, H. A. Gasteiger and R. J. Behm, *J. Electroanal. Chem.*, 2001, **495**, 134.
18. J. A. Poirier and G. E. Stoner, *J. Electrochem. Soc.*, 1994, **141**, 425.
19. J. Jiang and A. Kucernak, *Electrochem. Solid-State Lett.*, 2000, **3**, 559.
20. A. Saramat, M. Andersson, S. Hant, P. Thormählen, M. Skoglundh, G. S. Attard and A. E. C. Palmqvist, *Eur. Phys. J. D*, 2007, **43**, 209.